Identification of an acid sphingomyelinase ceramide kinase pathway in the regulation of the chemokine CCL5[S]

Benjamin Newcomb,[1,*] Cosima Rhein,[1,*,†] Izolda Mileva,* Rasheed Ahmad,[§] Christopher J. Clarke,* Justin Snider,* Lina M. Obeid,*,** and Yusuf A. Hannun*,**,[2]

Stony Brook Cancer Center* and the Department of Medicine,** Stony Brook University, Stony Brook, NY 11794, Department of Psychiatry and Psychotherapy,[†] University Hospital, Friedrich-Alexander University Erlangen-Nürnberg (FAU), 91054 Erlangen, Germany, Immunology and Innovative Cell Therapy Unit,[§] Dasman Diabetes Institute, Kuwait City, Kuwait

Abstract Acid sphingomyelinase (ASM) hydrolyzes sphingomyelin to produce the biologically active lipid ceramide. Previous studies have implicated ASM in the induction of the chemokine CCL5 in response to TNF-α; however, the lipid mediator of this effect was not established. In the present study, we identified a novel pathway connecting ASM and ceramide kinase (CERK). The results show that TNF-α induces the formation of ceramide 1-phosphate (C-1-P) in a CERK-dependent manner. Silencing of CERK blocks CCL5 production in response to TNF-α. Interestingly, cells lacking ASM have decreased C-1-P production following TNF-α treatment, suggesting that ASM may be acting upstream of CERK. Functionally, ASM and CERK induce a highly concordant program of cytokine production and both are required for migration of breast cancer cells. Taken together, these data suggest ASM can produce ceramide which is then converted to C-1-P by CERK, and that C-1-P is required for production of CCL5 and several cytokines and chemokines, with roles in cell migration. These results highlight the diversity in action of ASM through more than one bioactive sphingolipid.—Newcomb, B., C. Rhein, I. Mileva, R. Ahmad, C. J. Clarke, J. Snider, L. M. Obeid, and Y. A. Hannun. **Identification of an acid sphingomyelinase ceramide kinase pathway in the regulation of the chemokine CCL5.** *J. Lipid Res.* 2018. **59:** **1219–1229.**

Bioactive sphingolipids are a diverse group of signaling molecules that includes ceramide, sphingosine, ceramide 1-phosphate (C-1-P), and sphingosine 1-phosphate, with more than 40 metabolic enzymes that generate, catabolize, or interconvert them (1–7). Due to the large number of bioactive lipids and enzymes involved, the sphingolipid metabolic network is highly regulated and compartmentalized within the cell (8–10). Sphingolipid metabolism can be segregated into the de novo, hydrolytic, and salvage pathways. Sphingomyelin and other complex sphingolipids form the substrates for the sphingolipid hydrolytic and salvage pathways. Catabolism of sphingomyelin is mediated by the activity of the sphingomyelin phosphodiesterases, which generate ceramide, and subsequent metabolism of ceramide can generate sphingosine (11). Ceramide can also serve as a substrate for the formation of C-1-P through the action of ceramide kinase (CERK) (12). Ceramide has been implicated in multiple cellular functions, including apoptosis, response to chemotherapeutics, and other anti-mitogenic activities. In contrast, C-1-P has many important signaling functions in the mediation of several inflammatory processes that promote tumor formation and progression (6, 13, 14). Therefore, CERK may have a dual function in tumor promotion involving both the production of mitogenic C-1-P as well as clearance of apoptotic ceramide (15).

Previous work from our laboratory and others has revealed a pro-inflammatory role for the sphingolipid salvage pathway, with a particular focus on acid sphingomyelinase (ASM) (16–19). ASM is a 631 amino acid protein, encoded by the *SMPD1* gene. It mediates several downstream signaling responses initiated by lipopolysaccharides, oxidative stress, ionizing radiation, IL-1β, TNF-α, and phorbol 12-myristate 13-acetate, including roles in induction of protein kinase C, IL-6, and interferon γ (INF-γ) (20–23). ASM has also been implicated in viral and bacterial uptake and infection (24, 25). In particular, our previous studies disclosed an important role for ASM in mediating the induction of CCL5/RANTES in response to the action of IL-1 and TNF-α. CCL5 has been implicated as a key chemokine in the regulation of the tumor microenvironment, and along with

Abbreviations: ACD, acid ceramidase; ASM, acid sphingomyelinase; CERK, ceramide kinase; C-1-P, ceramide 1-phosphate; EMT, epithelial to mesenchymal transition; LN, Lesch-Nyhan; NPD, Niemann-Pick disease types A and B.

[1] Both authors contributed equally to this work.

[2] To whom correspondence should be addressed.

e-mail: yusuf.hannun@stonybrookmedicine.edu

[S] The online version of this article (available at http://www.jlr.org) contains a supplement.

other cytokines, including TNF-α, has been implicated in tumor progression and development of intratumoral heterogeneity (26–29). In breast cancer cells, TNF-α induces not only CCL5, but also NFkB, MAPK/AKT, AP1, JNK, Ras, as well as many other mitogenic pathways (30–33).

Interestingly, C-1-P and CERK are known to play roles in many of the same pathways induced by TNF-α and regulated by ASM. In nonsmall cell lung cancer cell lines, C-1-P has been found to be a potent activator of invasion and of MAKP and AKT signaling (34). Furthermore, CERK has been found to modulate NFkB activity in neutrophils from the lungs of mice challenged with lipopolysaccharides (35). In addition to its role as a modulator of stress responses in lung tissues, CERK has been found to activate stress-activated protein kinase/c-Jun N-terminal kinase and regulate lipid droplet formation in an ERK- and p38-independent manner (36). CERK is also known to have a direct role in TNF-α signaling. CERK has been shown to be a downstream modulator of TNF-α-induced cytosolic phospholipases A2 and in induction of NADPH oxidase (37, 38).

Due to the findings that ASM mediates inflammatory signaling in breast cancers, CERK promotes tumor progression, and CCL5 has a prominent role in the tumor microenvironment, we sought to investigate a possible connection between ASM, CERK, and CCL5. This was further prompted by an inability to pinpoint the role of ASM in mediating CCL5 on ceramide, sphingosine, or sphingosine 1-phosphate. Here, we present results that suggest that C-1-P mediates the production of CCL5 in response to TNF-α stimulation, and that CERK generates C-1-P from ceramide produced by ASM.

MATERIALS AND METHODS

Materials

MCF7 cells were obtained from ATCC (Manassas, VA). Niemann-Pick disease types A and B (NPD) (Cat GM16195, passage 11) and Lesch-Nyhan (LN) (Cat GM02226, passage 16) cells were obtained from Coriell Cell Repository (Camden, NJ). Trypsin-EDTA (0.05%) was from Gibco (Holtsville, NY, Cat 25300062). TNF-α was purchased from Peprotech (Rocky Hill, NJ). Porcine brain sphingomyelin was from Avanti Polar Lipids (Alabaster, AL, Cat 860062P).

Cell culture

MCF7 cells were maintained in RPMI from Gibco (Holtsville, NY, Cat 11875-093) supplemented with 10% (v/v) heat-inactivated FBS from HyClone (Port Washington, NY, Cat SH30396.03). MCF7 cells were kept in culture for no longer than 30 days. All cell lines were tested monthly for mycoplasma contamination using the MycoAlert kit from Lonza (Allendale, NJ, Cat LT07-218). NPD and LN cells were maintained at less than 75% confluency. All cell treatments with TNF-α were carried out in serum free media, unless otherwise noted.

Plasmids and transient transfection

The CERK-DsRed plasmid was a kind gift of Charles Chalfant. Generation of the pEF6-ASM-V5 plasmid was described previously (39). Transient transfections were carried out in 6-well trays with 1×10^5 cells per well. 24 h after seeding cells, the media were changed and cells were transfected with 1 µg of plasmid DNA per well, using X-tremeGENE DNA transfection reagent from Roche (Basel, Switzerland, Cat 06365787001) according to manufacturer's instructions.

RNA Interference

Small interfering RNA (siRNA) duplexes were obtained from ThermoScientific (Rockford, IL), and were designed against the following target sequences: ASM, 5′-AACTCCTTTGGATGGG-CCTGG-3′; and CERK (prevalidated, s34929). All-Star Negative Control siRNA was obtained from Qiagen. A total of 5×10^5 cells was plated in each well of a 6-well tray and 20 nM siRNA was transfected using Lipofectamine RNAiMAX from ThermoFisher (Cat 13778150), according to manufacturer's specifications. After 24 h, RNAi complexes were washed out, and cells were incubated with complete media for another 24 h. Media were exchanged 4 h prior to experimental manipulation.

ELISA

Sandwich ELISA kits for Human CCL5 were obtained from R&D Systems (Minneapolis, MN, Cat DY278-05 and DY008) and used according to the manufacturer's specifications. Briefly, cell supernatants were harvested, and centrifuged for 5 min at 21,000 g in a table top microcentrifuge, and 100 µL of supernatant was used per well of the ELISA assay. Cell lysates were prepared in buffer containing 50 mM TrisHCl, 0.2% TritonX-100, and protease inhibitor from Sigma (St. Louis, MO, Cat S8830-20TAB) (cell lysis buffer). Cell lysates were adjusted to a protein concentration of 0.5 mg/ml, and 100 µL of lysate was applied to each well of the ELISA.

Real time RT-PCR

RNA purification was performed with the Purelink RNA Kit from ThermoFisher, according to manufacturer's protocol. Concentration of RNA was determined by nanodrop, and 500 ng of RNA was transformed into cDNA using the Quanta cDNA Kit (Gaithersburg, MD, Cat 95047) according to the manufacturer's protocol. For RT-PCR, reactions were performed in triplicate in 96-well plates with each reaction containing 10 µl 2 × iTAQ mastermix, 5 µl of diluted (1:10, v/v) cDNA, 1 µl of 20× FAM tagged Taqman gene specific primer probe, 0.3 µL of 60× VIC tagged Actin probe, and 4 µl of water. The following probes were purchased from Life Technologies: ACTB (Cat Hs01060665_g1); ASM (Cat Hs03679347_g1); CERK (Cat Hs00368483_m1); CCL5 (Cat Hs00174575_m1).

Cytokine array

MCF7 cells were plated in 10 cm dishes at 10^5 cells per plate. The following day, cells were transfected with the plasmids containing overexpression vectors with the indicated genes. Cells were incubated for an additional 24 h. Cells were lysed, and mRNA was harvested and converted to cDNA as above. Cytokine arrays were obtained from SA Biosciences (Cat PAHS-150Z) and used according to manufacturer's protocol. Data were analyzed using the SA Biosciences PCR Array Data Analysis Software.

Sphingolipidomic analysis

MCF7 or NPD or LN cells were seeded at 10^6 cells per plate in 10 cm plates. Following 24 h of growth in complete media, cells were treated as indicated. Following treatment, cells were scraped and pelleted in cold PBS, and lipids were extracted in 2 ml isopropanol:water:ethyl acetate (30:10:60 by vol). Cell extracts were analyzed by reverse phase high pressure liquid chromatography coupled to electrospray ionization and subsequent separation by mass spectrometry. Analysis of sphingoid bases, ceramides, and sphingomyelins was performed on a Thermo Quantum Ultra

mass spectrometer, operating in a multiple reaction-monitoring positive ionization mode, as described (40). Lipid phosphate concentrations were measured and sphingolipid levels were normalized to total lipid phosphate in each sample.

In vitro ASM activity assay

ASM assays were performed as previously described (20). In brief, 200 μM porcine brain sphingomyelin was mixed with ^{14}C labeled sphingomyelin and Triton X-100. Micelles were formed by sonication in a buffer containing 250 mM sodium acetate (pH 5.00) and 1.0 mM EDTA. Cells were lysed in buffer containing 50 mM TrisHCl pH7.4, 0.2% Triton X-100, 1.0 mM EDTA, and protease inhibitor. An amount of 25 μg of cell lysate in 100μL lysis buffer was added to 100 μL of micelle mix and the reaction was incubated at 37°C for 30 min. The reaction was terminated with the addition of 1.5 ml of CHCl3: MeOH (2:1, v/v) followed by 0.4 ml of water. Samples were vortexed, centrifuged (5 min at 1,865 *g* in a table top centrifuge), and 0.8 ml of the aqueous/methanolic phase was removed for scintillation counting.

Transwell migration assay

Invasion of cells was measured using the Corning BioCoat Tumor Invasion System (Cat 354165), according to manufacturer's protocol. Briefly, MDA-MB-231 cells were trypsinized, and resuspended in serum free media at a concentration of 5×10^4 cells/ml. A total of 500 μL of cell suspension was added to the upper well of each chamber of the transwell plate. The lower chamber contained serum free media (control), complete media, or complete media plus TNF-α. Cells were allowed to invade for 48 h, and invasion of live cells was quantified by staining cells with Calcein AM and measuring fluorescence using a Spectra Max M5 mulitplate reader.

MTT assay

MDA-231 (100K) were reverse transfected with All Star or CERK siRNA (20nM) in 6-well trays for 24 h. To initiate the time course, media were changed and viable cell number was assessed by MTT assay at 0, 24, 48 and 72 h. Briefly, 1 ml of 5 mg/ml MTT was added to 1 ml media and incubated for 30 min at 37°C. Media were aspirated and formazan dye was solubilized in 2 ml DMSO for 10 min at room temperature with gentle rocking. Absorbance of formazan product was assessed at 570 nm.

Statistical analysis

Data are represented as the mean of at least three independent replicates ± standard error, unless otherwise indicated. Unpaired Student's *t*-test, one-way ANOVA with Dunnett's post test, and two-way ANOVA with Bonferroni post test statistical analyses were performed using Prism 6.2 software.

RESULTS

TNF-α induces C-1-P and CCL5 production

Previously, we demonstrated a role for ASM in IL-1β− and TNF-α− induced CCL5 production in MCF7 breast carcinoma cells (16). However, in these studies the functional sphingolipid mediating those actions was not defined. Because inflammatory cytokines are known to activate CERK to induce C-1-P (37, 41), we sought to investigate the role of CERK and C-1-P in CCL5 production and clarify the interactions between ASM and C-1-P.

As expected, we observed a rapid and robust time-dependent increase in the level of CCL5 following TNF-α treatment. CCL5 message increased up to 18-fold over control, (**Fig. 1A**) and secreted CCL5 protein increased up to 120-fold

over control (Fig. 1B) in response to TNF-α treatment (it should be noted, however, that the fold changes varied between experiments, mostly related to differences in the basal levels of CCL5). To investigate the possibility that C-1-P plays a role in the TNF-α response, we measured C-1-P levels following TNF-α stimulation, and observed a robust time dependent increase in C-1-P (Fig. 1C). Interestingly, sphingosine did not increase during TNF-α treatment (Fig. 1D, E). These data suggest TNF-α induces a C-1-P dependent signaling pathway in MCF7 cells in a relevant time frame.

To date, CERK is the only identified source of C-1-P in mammalian cells (42). As such, we sought to determine the role of CERK in production of C-1-P and CCL5. Using siRNA directed toward CERK, we were able to knock down expression of CERK (supplemental Fig. S1), and consequently, we measured a significant decrease in both the basal and TNF-α stimulated levels of C-1-P (**Fig. 2A**). To rule out a possible effect on ceramide and sphingosine levels, we measured both ceramide and sphingosine in vehicle- and TNF-α- treated cells. TNF-α induced a significant accumulation of ceramide that was not affected by ablation of CERK, albeit, there was a trend to an increase in ceramide levels that did not reach statistical significance (Fig. 2B). Additionally, CERK knockdown did not affect sphingosine levels in these cells (Fig. 2C). These data demonstrate that the increase in C-1-P in response to TNF-α is due to CERK activity, and that CERK knockdown does not affect levels of the related bioactive lipids, including ceramide and sphingosine.

CERK is required for CCL5 production

Cytokines, including CCL5, are regulated at many levels, including transcription, translation, and secretion (43–45). As such, we investigated the role of CERK in CCL5 production by measuring secreted CCL5 protein by ELISA. We observed that knockdown of CERK significantly reduced levels of CCL5 in the media of TNF-α-treated MCF7 cells (**Fig. 3A**). To assess the role of CERK in CCL5 expression, CCL5 mRNA was measured in cells treated with CERK siRNA. The results showed that ablation of CERK caused a significant decrease in the expression of the CCL5 message after treatment with TNF-α, commensurate with the effects on protein levels (Fig. 3B). Previous reports have shown that CCL5 is highly regulated at the secretory level, and that CCL5 is stored in secretory vesicles and vesicular fusion and subsequent CCL5 secretions are regulated by SNARE and synaptobrevin-2 (43, 46). To investigate whether CERK exerted a differential effect on CCL5 production vs. secretion, we compared secreted CCL5 to CCL5 within cells. The results showed that ablation of CERK reduced both secreted and cellular CCL5 after treatment with TNF-α (Fig. 3C, D), suggesting that CERK primarily regulates the production of CCL5 in MCF7 cells.

CERK is sufficient to induce CCL5

To investigate whether CERK is sufficient to induce CCL5, we transiently overexpressed CERK in MCF7 cells. CERK overexpression induced a significant increase in C-1-P levels compared with control (**Fig. 4A**). Functionally, CERK overexpression induced CCL5 mRNA levels (Fig. 4B)
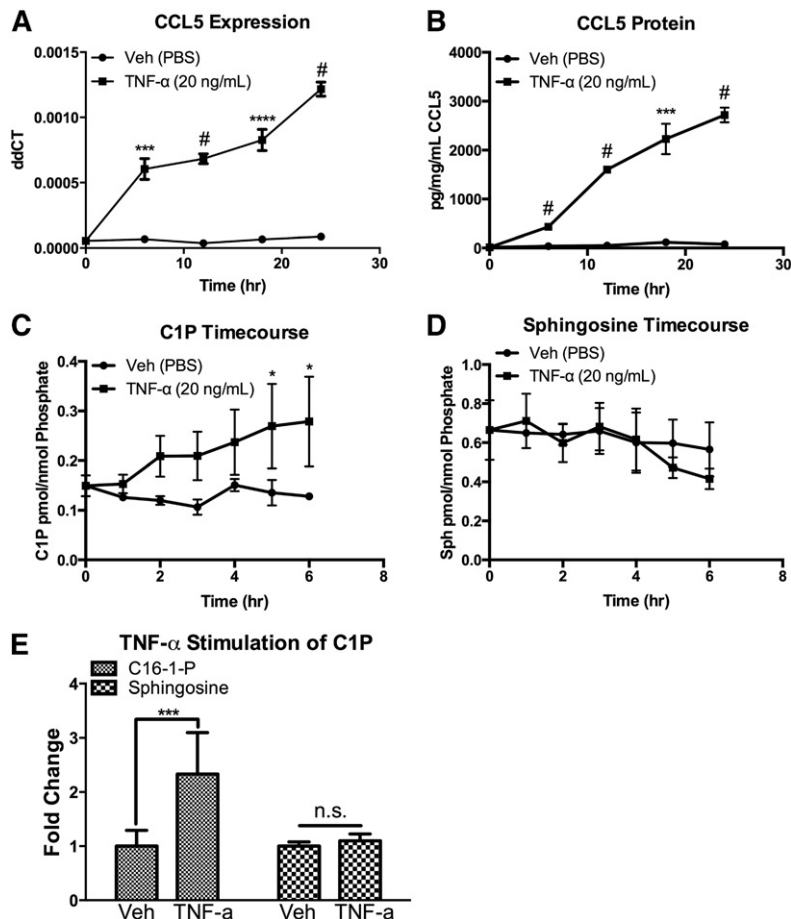
Fig. 1. TNF-α induces a CERK/C-1-P dependent pathway in MCF7 cells. MCF7 breast carcinoma cells were treated with vehicle (PBS) or TNF-α (20 ng/ml) for the indicated times. A: CCL5 mRNA levels were quantified by RTPCR, and (B) secretion into the media was measured by ELISA. C: Lipids were harvested from MCF7 cells treated with vehicle (PBS) or TNF-α (20 ng/ml) for the indicated time points. C-1-P was measured and normalized to total cellular lipid phosphate. D: Lipids were harvested from MCF7 cells treated with vehicle (PBS) or TNF-α (20 ng/ml) for the indicated time points. Sphingosine was measured and normalized to total cellular lipid phosphate. E: Lipids were harvested from MCF7 cells treated with vehicle (PBS) or TNF-α (20 ng/ml) for 18 h. C-1-P and sphingosine were measured and normalized to total cellular lipid phosphate. n = 3;* $P < 0.05$; *** $P < 0.005$; **** $P < 0.001$; # $P < 0.0005$. n.s., nonsignificant.

and a profound increase in secreted CCL5 (Fig. 4C). These data suggest that C-1-P is sufficient to induce CCL5 in MCF7 cells.

ASM is required for C-1-P production

Previous data demonstrated a role for ASM in the induction of CCL5 by IL-1β and TNF-α. Therefore, we sought to determine whether a metabolic connection exists between ASM-derived ceramide and C-1-P, or whether these were independently operating metabolic pathways. The results showed that TNF-α treatment caused a rapid increase in ASM activity (**Fig. 5A**), and, correspondingly, TNF-α-induced ceramide accumulation was also ASM dependent (Fig. 5B). The increases in ceramide and C-1-P following TNF-α stimulation are temporally related, suggesting the possibility that CERK utilizes ASM-derived ceramide to
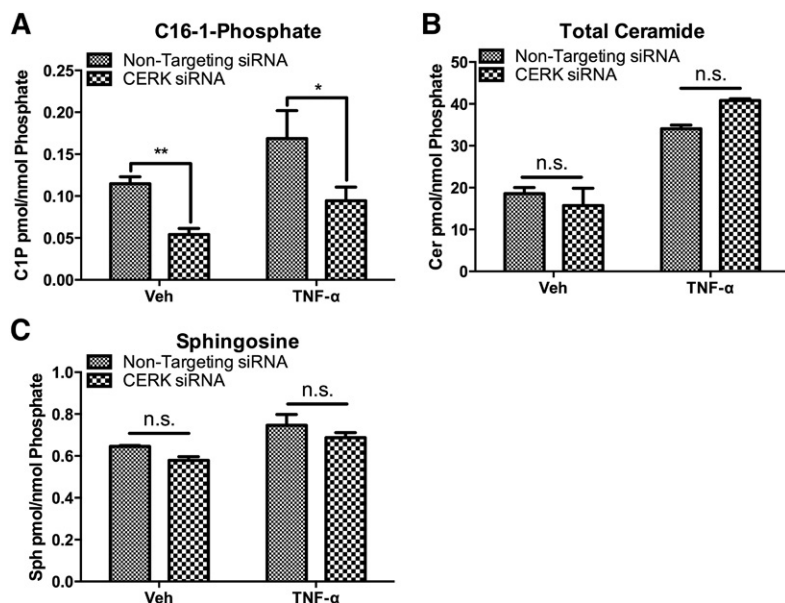

Fig. 2. Effect of CERK knockdown on lipid levels of C-1-P, ceramide, and sphingosine. MCF7 cells were treated with nontargeting (All Star) siRNA or CERK siRNA for 48 h prior to treatment with vehicle (PBS) or TNF-α for 18 h. :A: C-1-P, (B) ceramide, and (C) sphingosine levels were analyzed and normalized to total lipid phosphate. n = 3; * $P < 0.05$; ** $P < 0.01$. n.s., nonsignificant.
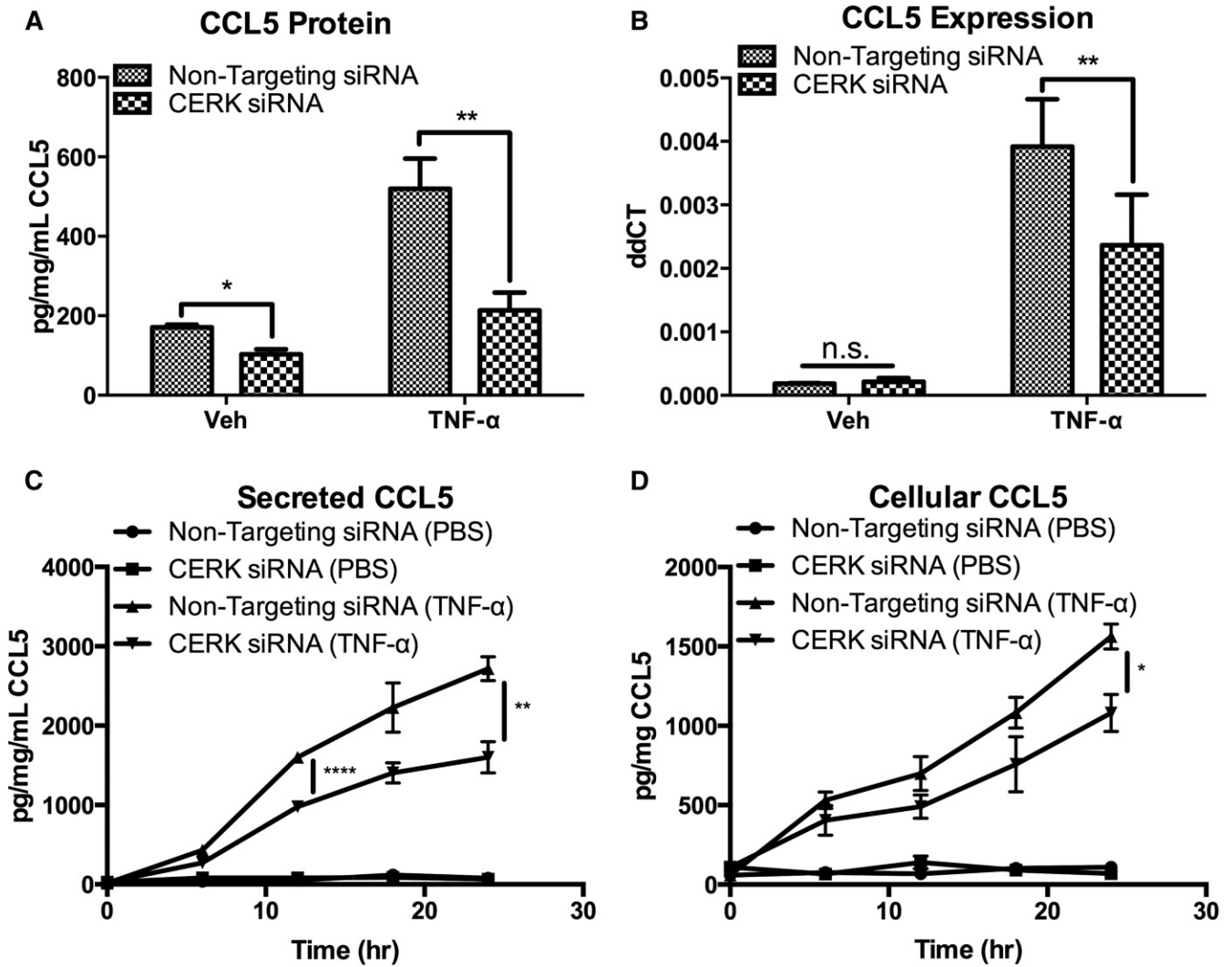
Fig. 3. CERK is required for CCL5 production in MCF7 cells. MCF7 cells were treated with nontargeting siRNA or CERK siRNA for 48 h prior to treatment with vehicle (PBS) or TNF-α (20 ng/ml). A: CCL5 secretion was measured after 18 h of TNF-α, and (B) CCL5 mRNA levels were measured after 6 h of TNF-α treatment. CCL5 protein levels were also measured in the (C) media and in (D) cells at the indicated time points. n = 3; * $P < 0.05$; ** $P < 0.01$; *** $P < 0.005$.

produce C-1-P and induce CCL5 in response to inflammatory stimuli. Indeed, the results showed that knockdown of ASM also suppressed the levels of C-1-P (Fig. 5C), suggesting that ASM provides at least a component of the ceramide required for the action of CERK. Also, knockdown of ASM in the presence of overexpressed CERK resulted in significant attenuation of the C-1-P response (Fig. 5D). In a complementary approach to investigate the possible link between ASM and CERK, we used a genetic model of ASM deficiency. NPD is characterized by a significant decrease in ASM activity. Therefore, fibroblasts from NPD patients can be used as a model of ASM deficiency. Because NPD fibroblasts have a significant defect in lysosomal function, we obtained fibroblasts from LN patients as a control, as LN fibroblasts have perturbed lysosomal function but do not have deficiencies in ASM or other sphingolipid metabolic enzymes. Both cell lines are known to respond to TNF-α treatment, and NPD fibroblasts have a significant defect in CCL5 production (16, 46). Herein, the results

showed that TNF-α caused a significant increase in C-1-P in LN fibroblasts, but the ASM deficient NPD fibroblasts did not produce C-1-P in response to TNF-α (Fig. 5E). Therefore, the results suggest that C-1-P is produced from ASM-derived ceramide.

Both ASM and CERK are required for CCL5 production

To further investigate whether ASM and CERK are part of the same signaling pathway, we analyzed the interaction of both in regard to CCL5 production. First, ASM was knocked down in the presence of overexpressed CERK. Importantly, knockdown of ASM attenuated the induction of CCL5 expression at both the protein (**Fig. 6A**) and mRNA levels (Fig. 6B). Reciprocally, knockdown of CERK in the presence of ASM overexpression led to a decrease in CCL5 levels on the protein (Fig. 6C) and message levels (Fig. 6D). Taken together, these results demonstrate that at least part of the C-1-P formed by CERK arises from the
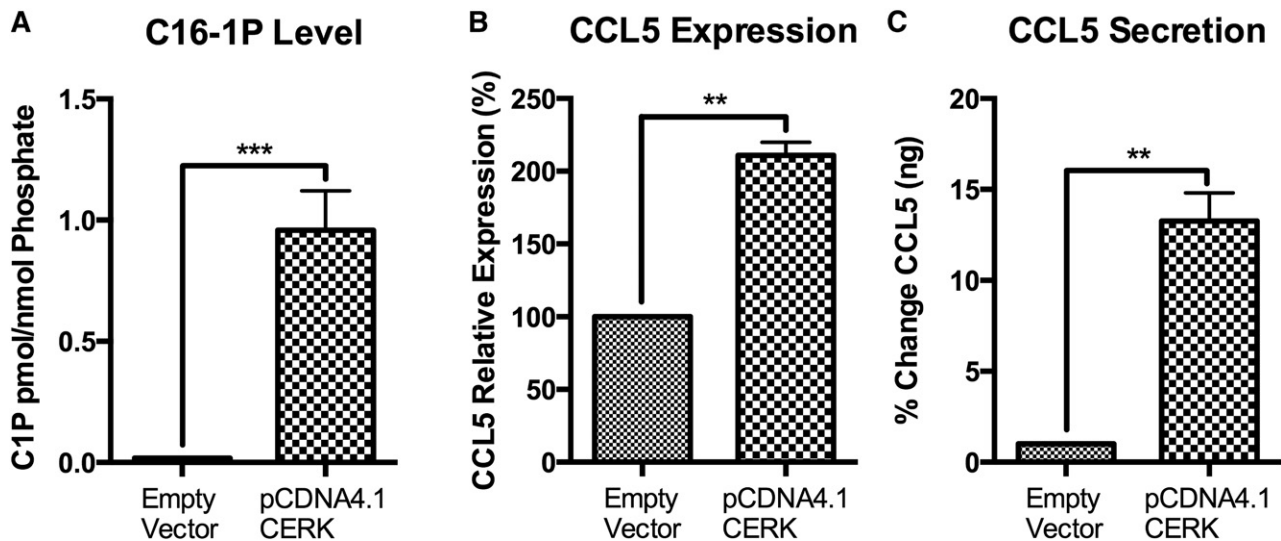
Fig. 4. Overexpression of CERK induces CCL5 in MCF7 cells. MCF7 cells were transfected with CERK over expression vector (CERK-DsRed) and compared with control condition. After 24 h, (A) C-1-P levels were measured and normalized to total lipid phosphate, (B) CCL5 message levels, and (C) CCL5 secretion were determined. A: n = 3; *** $P < 0.005$. B: n = 2; error bars represent range; ** $P < 0.01$. C: n = 2; error bars represent range; ** $P < 0.01$.

conversion of ceramide derived from ASM, and that this ceramide-C-1-P metabolic pathway is at least partly required for CCL5 production.

Role of the ASM/CERK signaling axis in cytokines associated with EMT, cell migration, and invasiveness

To analyze the extent of the cytokine response to ASM and CERK and to determine the overlap of ASM and CERK in cytokine regulation, we overexpressed ASM or CERK in MCF7 cells and conducted a quantitative RT-PCR cytokine array, which surveys 84 cytokines and chemokines. Overexpression of ASM resulted in the induction of 40 cytokines, whereas overexpression of CERK resulted in the induction of 27 cytokines. Twenty-six cytokines increased in common between ASM and CERK (**Fig. 7**). Low baseline expression of many of cytokines as well as experimental variability limits our ability to conclude on the significance of these results, however there is a strong trend toward a pro-inflammatory state in cells over expressing ASM and CERK. Many of the upregulated genes play roles in modulation of the tumor microenvironment and belonged to the TNF superfamily as well as a variety of pro-metastatic cytokines and interleukins. Of particular interest are several cytokines that are directly involved in the process of epithelial to mesenchymal transition (EMT), including TNF-α, IL-6, CCL5, and CCL2 (47–49). This indicates a common role for ASM and CERK in the regulation especially of those cytokines that are relevant for tumor progression. The precise roles for the individual cytokines and chemokines regulated by ASM and CERK remains to be determined in future studies. Interestingly, many of the assayed growth factors, such as VEGF and BMP2, were unaffected by overexpression of ASM/CERK. Furthermore, none of the assayed interferon genes were induced by ASM/CERK overexpression. This suggests the pathways induced by ASM/CERK are directly related to tumorigenesis and tumor spread.

Role of the ASM/CERK pathway in cancer cell migration

To investigate the biological role of the TNF-α-ASM-CERK pathway, we used a migration assay to analyze invasion in MDA-MB-231 breast carcinoma cells. MDA-MB-231 cells are highly metastatic and have a mesenchymal-like phenotype as well as a very high proportion of CD44+/CD24− cells (50). Using a Matrigel® Transwell® invasion system, the results showed that knockdown of either ASM or CERK resulted in profound inhibition of cell invasion (**Fig. 8A**). Inhibition of CERK did not alter the kinetics of cellular proliferation (supplemental Fig. S2). Thus, these results support an important role for the ASM/CERK pathway in the invasiveness of the postEMT breast cancer cell line MDA-MB-231.

DISCUSSION

Previous data have defined a role for ASM in the generation of ceramide following TNF-α stimulation and in the induction of CCL5 (51, 52). Here, we provide evidence that TNF-α induces a C-1-P dependent pathway that is sufficient and partly necessary to induce CCL5 (Fig. 8B). Additionally, CERK acts on ceramide produced by ASM, thus linking the activation of ASM and formation of ceramide to the production of C-1-P and CCL5. These data suggest that CERK is a master regulator of several inflammatory processes that can contribute to breast cancer progression.

The results from this study demonstrate a key role for C-1-P and CERK, the enzyme that generates it from ceramide, in regulation of CCL5 production. Knockdown of CERK led to a significant decrease in CCL5 mRNA and CCL5 protein following TNF-α stimulation. Furthermore, TNF-α caused a significant increase in C-1-P that correlated temporally with the increase in CCL5. In addition to being necessary for CCL5 production, overexpression of CERK was sufficient to induce CCL5. Taken together, these results
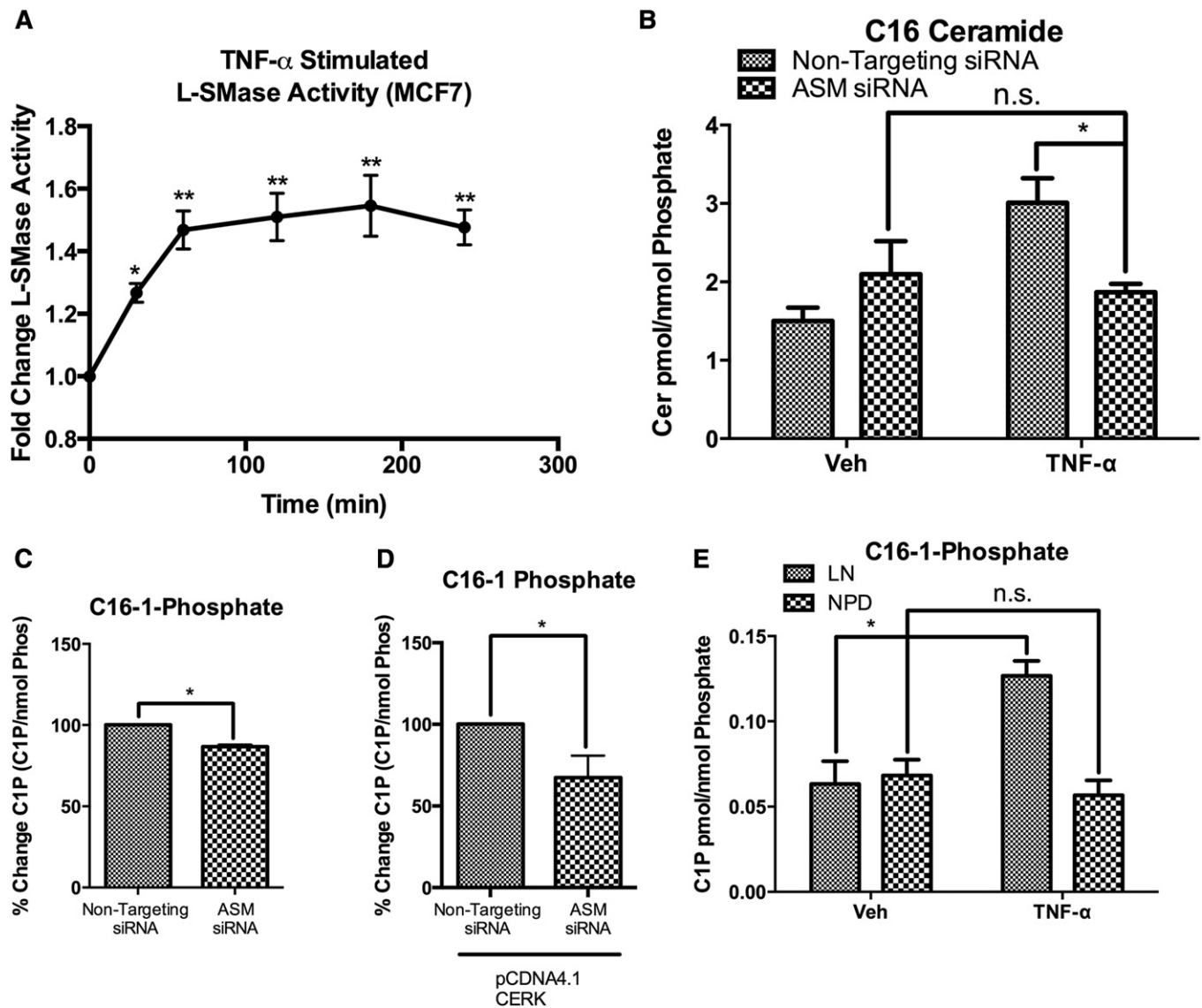
Fig. 5. CERK uses ASM derived ceramide to produce C-1-P. A: MCF7 cells were treated with TNF-α, and ASM activity was measured at the indicated time points. B: MCF7 cells were treated with nontargeting or ASM siRNA for 48 h, and then treated with vehicle (PBS) or TNF-α (20 ng/ml) for 18 h. C16-Ceramide levels and (C) C16-1-P levels were measured and normalized to total lipid phosphate. D: MCF7 cells were treated with nontargeting or ASM siRNA for 24 h, and then transfected with a CERK over expression vector for 24 h. C-1-P levels were measured and normalized to total lipid phosphate. E: Fibroblasts from patients with Lesch Nyhan (LN) or Nieman-Pick Disease (NPD) were treated with vehicle (PBS) or TNF-α (20 ng/ml) for 18 h. C-1-P levels were measured and normalized to total lipid phosphate. n = 3; * $P < 0.05$; ** $P < 0.01$. n.s., nonsignificant.

identify a novel function for CERK and C-1-P, in their regulation of CCL5.

Although ASM has been implicated in CCL5 production, the precise identity of the downstream bioactive lipid molecules has remained unclear. As sphingolipid metabolism constitutes a tightly-knit network of interconnected metabolites, the action of a specific enzyme (in this case, ASM) cannot be automatically attributed to its immediate product (ceramide in this case), because these metabolites are interconvertible. TNF-α stimulation of MCF7 cells induces both ASM activity and ceramide accumulation. Previous studies have demonstrated a role for acid ceramidase (ACD) in CCL5 production; however, sphingosine did not change in MCF7 cells treated with TNF-α. Nevertheless, there is a clear role for

ACD in CCL5 production and simultaneous ablation of both ACD and CERK results in an additive inhibition of CCL5 (data not shown). Taken together, these results suggest that ASM/CERK and ASM/ACD signaling pathways both regulate CCL5 through spatio-temporally distinct and cell type-dependent mechanisms. The finding that ASM is the major source of ceramide and C-1-P following TNF-α stimulation suggests that ASM is the rate-limiting source of ceramide in these stimulated breast cancer cells. As such, the results from this study clearly demonstrate that ASM is a regulator of the flux of ceramide through the CERK/C-1-P metabolic axis. Taken together, the results demonstrate that ASM/CERK may function, at least in the case of CCL5 induction, as a coupled metabolic pathway for formation of C-1-P (Fig. 8B).
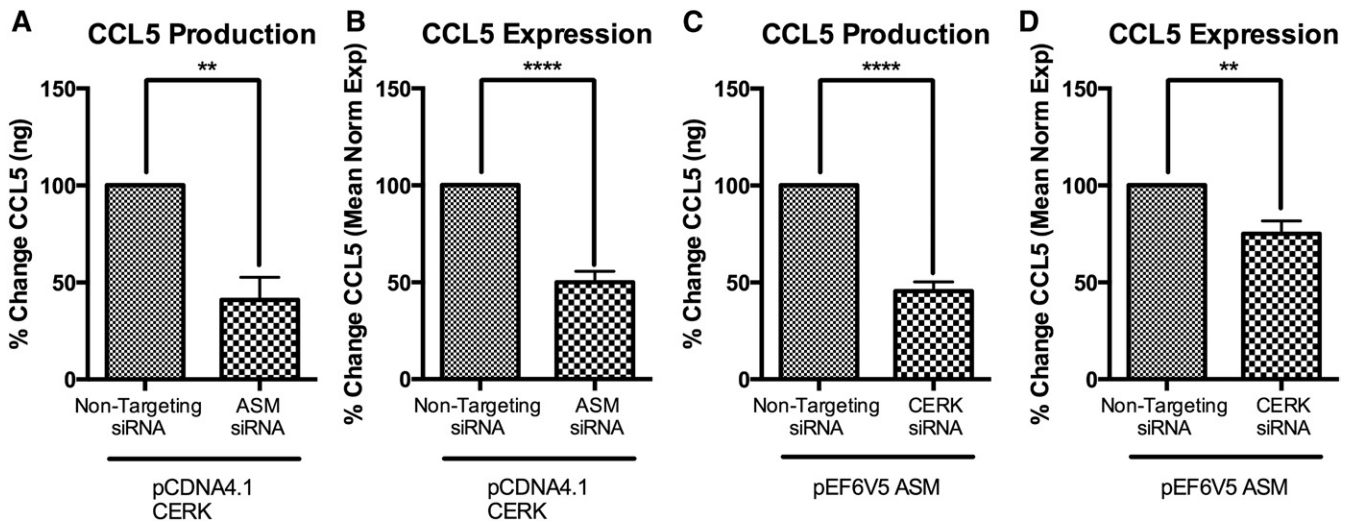
Fig. 6. ASM and CERK are required for CCL5 production. MCF7 cells were treated with nontargeting (All Star) or ASM siRNA for 24 h, and then transfected with a CERK over expression vector (CERK-DsRed) for 24 h. A: CCL5 protein levels, and CCL5 mRNA levels (B) were measured. C: MCF7 cells were treated with nontargeting (All Star) or CERK siRNA for 24 h, and then transfected with an ASM over expression vector (ASM-V5) for 24 h. CCL5 protein levels, and CCL5 mRNA levels (D) were measured. A: n = 3; ** $P < 0.01$. B–D: n = 4; ** $P < 0.01$; **** $P < 0.001$.

Defining a role for CERK in CCL5 production has helped elucidate the TNF-α induced CERK/C-1-P signaling cascade, and this provides novel insights into the role of C-1-P in inflammatory cytokine signaling in breast tumors. TNF-α has been shown to induce CERK activity and production of C1P in lung adenocarcinoma cells. This was
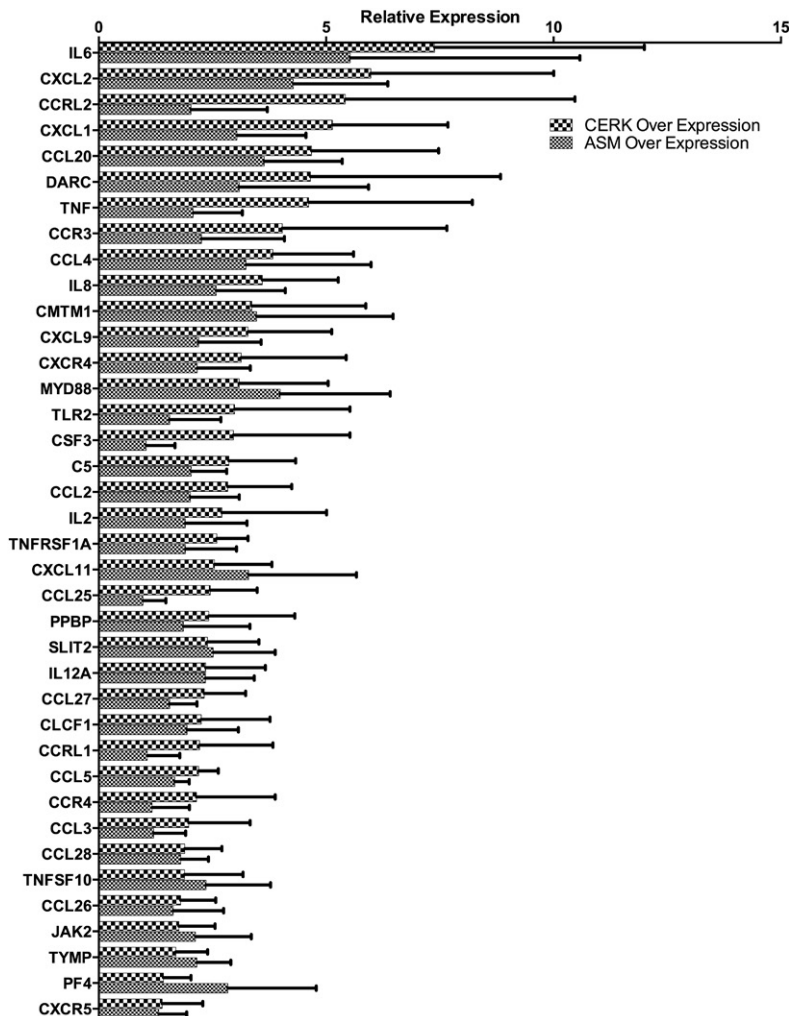

Fig. 7. ASM/CERK pathway regulates cytokine production in MCF7 cells. MCF7 cells were transfected with ASM or CERK over expression vectors. After 24 h of incubation, cDNA was prepared from the cells and cytokine expression was analyzed with TaqMan RTPCR cytokine arrays (n = 3).
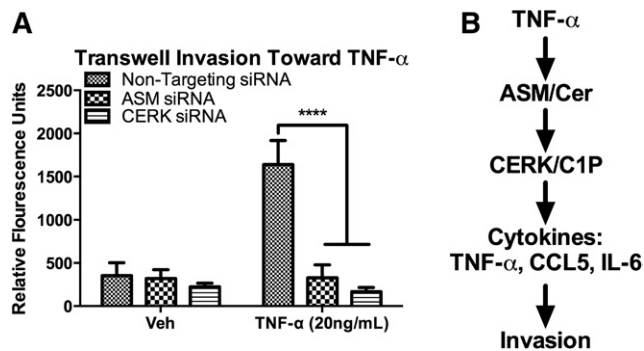
Fig. 8. ASM and CERK regulate cancer cell migration. A: MDA-MB-231 breast carcinoma cells were transfected with nontargeting (All Star) or ASM or CERK siRNA. After 48 h, cells were trypsinized and plated in the upper wells of Matrigel® Transwell ® invasion chambers. The lower well contained complete media with vehicle (PBS) or complete media with TNF-α (20 ng/ml). Cells were incubated for 48 h, and invasion was quantified by staining cells with calcein AM and measuring fluorescence. n = 3 in triplicate; **** $P<$ 0.001. B: Schematic representation of Cer/C1P signaling pathway.

implicated in the activation of cPLA2 and the production of prostaglandins in response to TNF-α (38). TNF-α was also shown to activate CERK in neuroblastoma cell lines; however, direct measurements of C-1-P were not always presented (37, 53). Our additional results also demonstrate that overexpression of CERK induces a plethora of cytokines and chemokines, all of which are known to be induced by TNF-α. The finding that TNF-α induces an accumulation of C-1-P supports the hypothesis that TNF-α is a potent inducer of CERK/C-1-P, and suggests that CERK may be an important part of the pro-inflammatory and signaling cascades induced by TNF-α.

These results have implications for breast cancer and its tumor microenvironment. In breast cancers, expression of both CERK and TNF-α is associated with poor outcomes (54–56). The microenvironment is shaped and defined by pro-inflammatory cytokines such as TNF-α, IL-1β, IL-6, and CCL5 (30, 57–60). These cytokines can promote survival of cancer stem-like cells, resistance to chemotherapeutics, and metastasis. Specifically, TNF-α and IL-1β are produced by infiltrating macrophages and lead to the formation of a feed-forward inflammatory cycle (61–64). In response to chronic TNF-α and IL-1β exposure, tumor cells and tumor-associated mesenchymal cells produce high levels of IL-6 and CCL5 (65, 66). Recent data highlighted the significance of CCL5 in tumor progression and poor outcomes in patients (67–70). CCL5 and its cognate receptor, CCR5, are known to be expressed in a coordinate and nonrandom manner in estrogen receptor negative breast carcinomas (70, 71). In addition, CCL5 was recently shown to foster a pro-tumor microenvironment and to activate STAT6- and ERK-mediated survival pathways (72). The finding that the CERK/C-1-P pathway is activated by TNF-α and results in the production of a large subset of inflammatory cytokines and chemokines may explain results demonstrating tumor progression in tumors expressing high levels of TNF-α (33). Therefore, targeting the CERK/C-1-P

signaling axis may have profound potential in the pharmacologic treatment of nonsurgical breast tumors.

Thus, coordinated expression of ASM and CERK may be a novel marker of tumor progression. These data may help to explain the previously reported paradoxical finding that high ceramide levels, which are usually connected with inducing apoptosis and growth suppression, are associated with poor outcomes in breast tumors (1), as the formation of C-1-P may dominate the cellular response. Additionally, ASM, previously also associated with apoptosis, is emerging as a key tumor promoter (73–75). In the pathway described in this study, elevated ceramide may serve as a precursor to higher C-1-P levels which may 'override' the cell intrinsic functions of ceramide by promoting inflammatory and other tumor-promoting effects. Our work supports a paradigm shift by demonstrating a strong pro-tumor role for ASM and TNF-α through a direct link between ASM and CERK (Fig. 8B).🔓

REFERENCES

1. Schiffmann, S., J. Sandner, K. Birod, I. Wobst, C. Angioni, E. Ruckhaberle, M. Kaufmann, H. Ackermann, J. Lotsch, H. Schmidt, et al. 2009. Ceramide synthases and ceramide levels are increased in breast cancer tissue. *Carcinogenesis.* **30:** 745–752.

2. Ruckhäberle, E., T. Karn, A. Rody, L. Hanker, R. Gatje, D. Metzler, U. Holtrich, and M. Kaufmann. 2009. Gene expression of ceramide kinase, galactosyl ceramide synthase and ganglioside GD3 synthase is associated with prognosis in breast cancer. *J. Cancer Res. Clin. Oncol.* **135:** 1005–1013.

3. Ramírez de Molina, A., A. de la Cueva, R. Machado-Pinilla, V. Rodriguez-Fanjul, T. Gomez del Pulgar, A. Cebrian, R. Perona, and J. C. Lacal. 2012. Acid ceramidase as a chemotherapeutic target to overcome resistance to the antitumoral effect of choline kinase alpha inhibition. *Curr. Cancer Drug Targets.* **12:** 617–624.

4. Korbelik, M., W. Zhang, K. M. Saw, Z. M. Szulc, A. Bielawska, and D. Separovic. 2013. Cationic ceramides and analogues, LCL30 and LCL85, as adjuvants to photodynamic therapy of tumors. *J. Photochem. Photobiol. B.* **126:** 72–77.

5. Hankins, J. L., K. E. Ward, S. S. Linton, B. M. Barth, R. V. Stahelin, T. E. Fox, and M. Kester. 2013. Ceramide 1-phosphate mediates endothelial cell invasion via the annexin a2-p11 heterotetrameric protein complex. *J. Biol. Chem.* **288:** 19726–19738.

6. Gangoiti, P., C. Bernacchioni, C. Donati, F. Cencetti, A. Ouro, A. Gomez-Munoz, and P. Bruni. 2012. Ceramide 1-phosphate stimulates proliferation of C2C12 myoblasts. *Biochimie.* **94:** 597–607.

7. Realini, N., C. Solorzano, C. Pagliuca, D. Pizzirani, A. Armirotti, R. Luciani, M. P. Costi, T. Bandiera, and D. Piomelli. 2013. Discovery of highly potent acid ceramidase inhibitors with in vitro tumor chemosensitizing activity. *Sci. Rep.* **3:** 1035.

8. Adada, M., C. Luberto, and D. Canals. 2016. Inhibitors of the sphingomyelin cycle: sphingomyelin synthases and sphingomyelinases. *Chem. Phys. Lipids.* **197:** 45–59.

9. Rovina, P., A. Schanzer, C. Graf, D. Mechtcheriakova, M. Jaritz, and F. Bornancin. 2009. Subcellular localization of ceramide kinase and ceramide kinase-like protein requires interplay of their Pleckstrin Homology domain-containing N-terminal regions together with C-terminal domains. *Biochim. Biophys. Acta.* **1791:** 1023–1030.

10. Lamour, N. F., R. V. Stahelin, D. S. Wijesinghe, M. Maceyka, E. Wang, J. C. Allegood, A. H. Merrill, Jr., W. Cho, and C. E. Chalfant. 2007. Ceramide kinase uses ceramide provided by ceramide transport protein: localization to organelles of eicosanoid synthesis. *J. Lipid Res.* **48:** 1293–1304.

11. Hannun, Y. A., and L. M. Obeid. 2018. Sphingolipids and their metabolism in physiology and disease. *Nat. Rev. Mol. Cell Biol.* **19:** 175–191.

12. Sugiura, M., K. Kono, H. Liu, T. Shimizugawa, H. Minekura, S. Spiegel, and T. Kohama. 2002. Ceramide kinase, a novel lipid kinase. Molecular cloning and functional characterization. *J. Biol. Chem.* **277:** 23294–23300.

13. Pettus, B. J., C. E. Chalfant, and Y. A. Hannun. 2004. Sphingolipids in inflammation: roles and implications. *Curr. Mol. Med.* **4:** 405–418.

14. Pastukhov, O., S. Schwalm, U. Zangemeister-Wittke, D. Fabbro, F. Bornancin, L. Japtok, B. Kleuser, J. Pfeilschifter, and A. Huwiler. 2014. The ceramide kinase inhibitor NVP-231 inhibits breast and lung cancer cell proliferation by inducing M phase arrest and subsequent cell death. *Br. J. Pharmacol.* **171:** 5829–5844.

15. Simanshu, D. K., X. Zhai, D. Munch, D. Hofius, J. E. Markham, J. Bielawski, A. Bielawska, L. Malinina, J. G. Molotkovsky, J. W. Mundy, et al. 2014. Arabidopsis accelerated cell death 11, ACD11, is a ceramide-1-phosphate transfer protein and intermediary regulator of phytoceramide levels. *Cell Reports.* **6:** 388–399.

16. Jenkins, R. W., C. J. Clarke, D. Canals, A. J. Snider, C. R. Gault, L. Heffernan-Stroud, B. X. Wu, F. Simbari, P. Roddy, K. Kitatani, et al. 2011. Regulation of CC ligand 5/RANTES by acid sphingomyelinase and acid ceramidase. *J. Biol. Chem.* **286:** 13292–13303.

17. Perry, D. M., B. Newcomb, M. Adada, B. X. Wu, P. Roddy, K. Kitatani, L. Siskind, L. M. Obeid, and Y. A. Hannun. 2014. Defining a role for acid sphingomyelinase in the p38/interleukin-6 pathway. *J. Biol. Chem.* **289:** 22401–22412.

18. Kitatani, K., K. Sheldon, V. Anelli, R. W. Jenkins, Y. Sun, G. A. Grabowski, L. M. Obeid, and Y. A. Hannun. 2009. Acid beta-glucosidase 1 counteracts p38delta-dependent induction of interleukin-6: possible role for ceramide as an anti-inflammatory lipid. *J. Biol. Chem.* **284:** 12979–12988.

19. Ali, M., A. Saroha, Y. Pewzner-Jung, and A. H. Futerman. 2015. LPS-mediated septic shock is augmented in ceramide synthase 2 null mice due to elevated activity of TNFalpha-converting enzyme. *FEBS Lett.* **589:** 2213–2217.

20. Jenkins, R. W., D. Canals, J. Idkowiak-Baldys, F. Simbari, P. Roddy, D. M. Perry, K. Kitatani, C. Luberto, and Y. A. Hannun. 2010. Regulated secretion of acid sphingomyelinase: implications for selectivity of ceramide formation. *J. Biol. Chem.* **285:** 35706–35718.

21. Zeidan, Y. H., and Y. A. Hannun. 2007. Activation of acid sphingomyelinase by protein kinase Cdelta-mediated phosphorylation. *J. Biol. Chem.* **282:** 11549–11561.

22. Zhu, H., K. Deng, Y. Q. Zhao, X. Wang, Y. L. Shen, T. G. Liu, D. D. Cui, and F. Xu. 2015. The effects of ASMase mediated endothelial cell apoptosis in multiple hypofractionated irradiations in CT26 tumor bearing mice. *Asian Pac. J. Cancer Prev.* **16:** 4543–4548.

23. Li, X., E. Gulbins, and Y. Zhang. 2012. Oxidative stress triggers Ca-dependent lysosome trafficking and activation of acid sphingomyelinase. *Cell. Physiol. Biochem.* 30: 815–826.

24. Grassmé, H., E. Gulbins, B. Brenner, K. Ferlinz, K. Sandhoff, K. Harzer, F. Lang, and T. F. Meyer. 1997. Acidic sphingomyelinase mediates entry of N. gonorrhoeae into nonphagocytic cells. *Cell.* **91:** 605–615.

25. Grassmé, H., V. Jendrossek, A. Riehle, G. von Kurthy, J. Berger, H. Schwarz, M. Weller, R. Kolesnick, and E. Gulbins. 2003. Host defense against Pseudomonas aeruginosa requires ceramide-rich membrane rafts. *Nat. Med.* **9:** 322–330.

26. Serrels, A., T. Lund, B. Serrels, A. Byron, R. C. McPherson, A. von Kriegsheim, L. Gomez-Cuadrado, M. Canel, M. Muir, J. E. Ring, et al. 2015. Nuclear FAK controls chemokine transcription, Tregs, and evasion of anti-tumor immunity. *Cell.* **163:** 160–173.

27. Bonapace, L., M. M. Coissieux, J. Wyckoff, K. D. Mertz, Z. Varga, T. Junt, and M. Bentires-Alj. 2014. Cessation of CCL2 inhibition accelerates breast cancer metastasis by promoting angiogenesis. *Nature.* **515:** 130–133.

28. Joyce, J. A., and D. T. Fearon. 2015. T cell exclusion, immune privilege, and the tumor microenvironment. *Science.* **348:** 74–80.

29. Marusyk, A., D. P. Tabassum, P. M. Altrock, V. Almendro, F. Michor, and K. Polyak. 2014. Non-cell-autonomous driving of tumour growth supports sub-clonal heterogeneity. *Nature.* **514:** 54–58.

30. Soria, G., M. Ofri-Shahak, I. Haas, N. Yaal-Hahoshen, L. Leider-Trejo, T. Leibovich-Rivkin, P. Weitzenfeld, T. Meshel, E. Shabtai, M. Gutman, et al. 2011. Inflammatory mediators in breast cancer: coordinated expression of TNFalpha & IL-1beta with CCL2 & CCL5 and effects on epithelial-to-mesenchymal transition. *BMC Cancer.* **11:** 130.

31. Leibovich-Rivkin, T., Y. Liubomirski, T. Meshel, A. Abashidze, D. Brisker, H. Solomon, V. Rotter, M. Weil, and A. Ben-Baruch. 2014. The inflammatory cytokine TNFalpha cooperates with Ras in elevating metastasis and turns WT-Ras to a tumor-promoting entity in MCF-7 cells. *BMC Cancer.* **14:** 158.

32. Rivas, M. A., R. P. Carnevale, C. J. Proietti, C. Rosemblit, W. Beguelin, M. Salatino, E. H. Charreau, I. Frahm, S. Sapia, P. Brouckaert, et al. 2008. TNF alpha acting on TNFR1 promotes breast cancer growth via p42/P44 MAPK, JNK, Akt and NF-kappa B-dependent pathways. *Exp. Cell Res.* **314:** 509–529.

33. Qiao, Y., H. He, P. Jonsson, I. Sinha, C. Zhao, and K. Dahlman-Wright. 2016. AP-1 is a key regulator of proinflammatory cytokine TNFalpha-mediated triple-negative breast cancer progression. *J. Biol. Chem.* **291:** 5068–5079.

34. Schneider, G., Z. P. Sellers, K. Bujko, S. S. Kakar, M. Kucia, and M. Z. Ratajczak. 2017. Novel pleiotropic effects of bioactive phospholipids in human lung cancer metastasis. *Oncotarget.* **8:** 58247–58263

35. Baudiß, K., R. de Paula Vieira, S. Cicko, K. Ayata, M. Hossfeld, N. Ehrat, A. Gomez-Munoz, H. K. Eltzschig, and M. Idzko. 2016. C1P attenuates lipopolysaccharide-induced acute lung injury by preventing NF-kappaB activation in neutrophils. Journal of immunology (Baltimore, Md.: 1950) 196: 2319–2326.

36. Gubern, A., M. Barcelo-Torns, D. Barneda, J. M. Lopez, R. Masgrau, F. Picatoste, C. E. Chalfant, J. Balsinde, M. A. Balboa, and E. Claro. 2009. JNK and ceramide kinase govern the biogenesis of lipid droplets through activation of group IVA phospholipase A2. *J. Biol. Chem.* **284:** 32359–32369.

37. Barth, B. M., S. J. Gustafson, J. L. Hankins, J. M. Kaiser, J. K. Haakenson, M. Kester, and T. B. Kuhn. 2012. Ceramide kinase regulates TNFalpha-stimulated NADPH oxidase activity and eicosanoid biosynthesis in neuroblastoma cells. *Cell. Signal.* **24:** 1126–1133.

38. Lamour, N. F., P. Subramanian, D. S. Wijesinghe, R. V. Stahelin, J. V. Bonventre, and C. E. Chalfant. 2009. Ceramide 1-phosphate is required for the translocation of group IVA cytosolic phospholipase A2 and prostaglandin synthesis. *J. Biol. Chem.* **284:** 26897–26907.

39. Bini, F., A. Frati, M. Garcia-Gil, C. Battistini, M. Granado, M. Martinesi, E. Mainardi, E. Vannini, F. Luzzati, M. Caleo, et al. 2012. New signalling pathway involved in the anti-proliferative action of vitamin D(3) and its analogues in human neuroblastoma cells. A role for ceramide kinase. *Neuropharmacology.* **63:** 524–537.

40. Bielawski, J., J. S. Pierce, J. Snider, B. Rembiesa, Z. M. Szulc, and A. Bielawska. 2010. Sphingolipid analysis by high performance liquid chromatography-tandem mass spectrometry (HPLC-MS/MS). *Adv. Exp. Med. Biol.* **688:** 46–59.

41. Pettus, B. J., A. Bielawska, S. Spiegel, P. Roddy, Y. A. Hannun, and C. E. Chalfant. 2003. Ceramide kinase mediates cytokine- and calcium ionophore-induced arachidonic acid release. *J. Biol. Chem.* **278:** 38206–38213.

42. Mitsutake, S., U. Yokose, M. Kato, I. Matsuoka, J. M. Yoo, T. J. Kim, H. S. Yoo, K. Fujimoto, Y. Ando, M. Sugiura, et al. 2007. The generation and behavioral analysis of ceramide kinase-null mice, indicating a function in cerebellar Purkinje cells. *Biochem. Biophys. Res. Commun.* **363:** 519–524.

43. Frank, S. P., K. P. Thon, S. C. Bischoff, and A. Lorentz. 2011. SNAP-23 and syntaxin-3 are required for chemokine release by mature human mast cells. *Mol. Immunol.* **49:** 353–358.

44. Lim, J. K., J. M. Burns, W. Lu, and A. L. DeVico. 2005. Multiple pathways of amino terminal processing produce two truncated variants of RANTES/CCL5. *J. Leukoc. Biol.* **78:** 442–452.

45. Hoffmann, A., A. Levchenko, M. L. Scott, and D. Baltimore. 2002. The IkappaB-NF-kappaB signaling module: temporal control and selective gene activation. *Science.* **298:** 1241–1245.

46. Lacy, P., M. R. Logan, B. Bablitz, and R. Moqbel. 2001. Fusion protein vesicle-associated membrane protein 2 is implicated in IFN-gamma-induced piecemeal degranulation in human eosinophils from atopic individuals. *J. Allergy Clin. Immunol.* **107:** 671–678.

47. Kuno, K., K. Sukegawa, Y. Ishikawa, T. Orii, and K. Matsushima. 1994. Acid sphingomyelinase is not essential for the IL-1 and tumor necrosis factor receptor signaling pathway leading to NFkB activation. *Int. Immunol.* **6:** 1269–1272.

48. Li, C. W., W. Xia, L. Huo, S. O. Lim, Y. Wu, J. L. Hsu, C. H. Chao, H. Yamaguchi, N. K. Yang, Q. Ding, et al. 2012. Epithelial-mesenchymal transition induced by TNF-alpha requires NF-kappaB-mediated transcriptional upregulation of Twist1. *Cancer Res.* **72:** 1290–1300.

49. Chen, W., Q. Gao, S. Han, F. Pan, and W. Fan. 2015. The CCL2/CCR2 axis enhances IL-6-induced epithelial-mesenchymal transition

by cooperatively activating STAT3-Twist signaling. *Tumour Biol.* **36:** 973–981.

50. Zhang, B., C. Yin, H. Li, L. Shi, N. Liu, Y. Sun, S. Lu, Y. Liu, L. Sun, X. Li, W. Chen, and Y. Qi. 2013. Nir1 promotes invasion of breast cancer cells by binding to chemokine (C-C motif) ligand 18 through the PI3K/Akt/GSK3beta/Snail signalling pathway. European journal of cancer (Oxford, England: 1990) 49: 3900–3913.

51. Wang, R., Q. Lv, W. Meng, Q. Tan, S. Zhang, X. Mo, and X. Yang. 2014. Comparison of mammosphere formation from breast cancer cell lines and primary breast tumors. *J. Thorac. Dis.* **6:** 829–837.

52. Novgorodov, S. A., D. A. Chudakova, B. W. Wheeler, J. Bielawski, M. S. Kindy, L. M. Obeid, and T. I. Gudz. 2011. Developmentally regulated ceramide synthase 6 increases mitochondrial Ca2+ loading capacity and promotes apoptosis. *J. Biol. Chem.* **286:** 4644–4658.

53. Sawai, H., H. Ogiso, and T. Okazaki. 2015. Differential changes in sphingolipids between TNF-induced necroptosis and apoptosis in U937 cells and necroptosis-resistant sublines. *Leuk. Res.* **39:** 964–970.

54. Saglam, S., R. Suzme, and F. Gurdol. 2009. Serum tumor necrosis factor-alpha and interleukin-2 concentrations in newly diagnosed ERBB2 (HER2/neu) positive breast cancer patients. *Int. J. Biol. Markers.* **24:** 142–146.

55. Omair, M. A., V. Phumethum, and S. R. Johnson. 2012. Long-term safety and effectiveness of tumour necrosis factor inhibitors in systemic sclerosis patients with inflammatory arthritis. *Clin. Exp. Rheumatol.* **30:** S55–S59.

56. Payne, A. W., D. K. Pant, T. C. Pan, and L. A. Chodosh. 2014. Ceramide kinase promotes tumor cell survival and mammary tumor recurrence. *Cancer Res.* **74:** 6352–6363.

57. Soria, G., and A. Ben-Baruch. 2008. The inflammatory chemokines CCL2 and CCL5 in breast cancer. *Cancer Lett.* **267:** 271–285.

58. Grivennikov, S. I., and M. Karin. 2011. Inflammatory cytokines in cancer: tumour necrosis factor and interleukin 6 take the stage. *Ann. Rheum. Dis.* **70(Suppl 1):** i104–i108.

59. Ponnusamy, S., M. Meyers-Needham, C. E. Senkal, S. A. Saddoughi, D. Sentelle, S. P. Selvam, A. Salas, and B. Ogretmen. 2010. Sphingolipids and cancer: ceramide and sphingosine-1-phosphate in the regulation of cell death and drug resistance. *Future Oncol.* **6:** 1603–1624.

60. Lv, D., Y. Zhang, H. J. Kim, L. Zhang, and X. Ma. 2013. CCL5 as a potential immunotherapeutic target in triple-negative breast cancer. *Cell. Mol. Immunol.* **10:** 303–310.

61. Wolczyk, D., M. Zaremba-Czogalla, A. Hryniewicz-Jankowska, R. Tabola, K. Grabowski, A. F. Sikorski, and K. Augoff. 2016. TNF-alpha promotes breast cancer cell migration and enhances the concentration of membrane-associated proteases in lipid rafts. *Cell Oncol. (Dordr.).* **39:** 353–363.

62. Futakuchi, M., K. Fukamachi, and M. Suzui. 2016. Heterogeneity of tumor cells in the bone microenvironment: Mechanisms and therapeutic targets for bone metastasis of prostate or breast cancer. *Adv. Drug Deliv. Rev.* **99:** 206–211.

63. Demirkan, B. 2013. The roles of epithelial-to-mesenchymal transition (EMT) and mesenchymal-to-epithelial transition (MET) in breast cancer bone metastasis: potential targets for prevention and treatment. *J. Clin. Med.* **2:** 264–282.

64. Banerjee, K., and H. Resat. 2016. Constitutive activation of STAT3 in breast cancer cells: a review. *Int. J. Cancer.* **138:** 2570–2578.

65. Juárez, P., and T. A. Guise. 2011. TGF-beta in cancer and bone: implications for treatment of bone metastases. *Bone.* **48:** 23–29.

66. Korkaya, H., S. Liu, and M. S. Wicha. 2011. Breast cancer stem cells, cytokine networks, and the tumor microenvironment. *J. Clin. Invest.* **121:** 3804–3809.

67. Niwa, Y., H. Akamatsu, H. Niwa, H. Sumi, Y. Ozaki, and A. Abe. 2001. Correlation of tissue and plasma RANTES levels with disease course in patients with breast or cervical cancer. Clinical cancer research: an official journal of the American Association for Cancer Research 7: 285–289.

68. Luboshits, G., S. Shina, O. Kaplan, S. Engelberg, D. Nass, B. Lifshitz-Mercer, S. Chaitchik, I. Keydar, and A. Ben-Baruch. 1999. Elevated expression of the CC chemokine regulated on activation, normal T cell expressed and secreted (RANTES) in advanced breast carcinoma. *Cancer Res.* **59:** 4681–4687.

69. Bièche, I., F. Lerebours, S. Tozlu, M. Espie, M. Marty, and R. Lidereau. 2004. Molecular profiling of inflammatory breast cancer: identification of a poor-prognosis gene expression signature. Clinical cancer research: an official journal of the American Association for Cancer Research 10: 6789–6795.

70. Velasco-Velázquez, M., X. Jiao, M. De La Fuente, T. G. Pestell, A. Ertel, M. P. Lisanti, and R. G. Pestell. 2012. CCR5 antagonist blocks metastasis of basal breast cancer cells. *Cancer Res.* **72:** 3839–3850.

71. Yaal-Hahoshen, N., S. Shina, L. Leider-Trejo, I. Barnea, E. L. Shabtai, E. Azenshtein, I. Greenberg, I. Keydar, and A. Ben-Baruch. 2006. The chemokine CCL5 as a potential prognostic factor predicting disease progression in stage II breast cancer patients. Clinical cancer research: an official journal of the American Association for Cancer Research 12: 4474–4480.

72. Zhang, Q., J. Qin, L. Zhong, L. Gong, B. Zhang, Y. Zhang, and W. Q. Gao. 2015. CCL5-mediated Th2 immune polarization promotes metastasis in luminal breast cancer. *Cancer Res.* **75:** 4312–4321.

73. Carpinteiro, A., N. Beckmann, A. Seitz, G. Hessler, B. Wilker, M. Soddemann, I. Helfrich, B. Edelmann, E. Gulbins, and K. A. Becker. 2016. Role of acid sphingomyelinase-induced signaling in melanoma cells for hematogenous tumor metastasis. *Cell. Physiol. Biochem.* 38: 1–14.

74. Carpinteiro, A., K. A. Becker, L. Japtok, G. Hessler, S. Keitsch, M. Pozgajova, K. W. Schmid, C. Adams, S. Muller, B. Kleuser, et al. 2015. Regulation of hematogenous tumor metastasis by acid sphingomyelinase. *EMBO Mol. Med.* **7:** 714–734.

75. Klutzny, S., R. Lesche, M. Keck, S. Kaulfuss, A. Schlicker, S. Christian, C. Sperl, R. Neuhaus, J. Mowat, M. Steckel, et al. 2017. Functional inhibition of acid sphingomyelinase by Fluphenazine triggers hypoxia-specific tumor cell death. *Cell Death Dis.* **8:** e2709.